Spontaneous Tumor Regression in Tasmanian Devils Associated with *RASL11A* Activation

Mark J. Margres,*,†,1 Manuel Ruiz-Aravena,‡ Rodrigo Hamede,‡,§ Kusum Chawla,,†† Austin H. Patton,* Matthew F. Lawrance,* Alexandra K. Fraik,* Amanda R. Stahlke,‡‡ Brian W. Davis,§§,*** Elaine A. Ostrander,*** Menna E. Jones,‡ Hamish McCallum,††† Patrick J. Paddison,** Paul A. Hohenlohe,‡‡ David Hockenbery,**,†† and Andrew Storfer***

*School of Biological Sciences, Washington State University, Pullman, Washington 99164, †Department of Organismic and Evolutionary Biology, Harvard University, Cambridge, Massachusetts 02138, ‡School of Natural Sciences, University of Tasmania, Hobart, Tasmania 7001, Australia, §Centre for Integrative Ecology, Deakin University, Waurn Ponds, Victoria 3216, Australia, **Division of Human Biology and ††Division of Clinical Research, Fred Hutchinson Cancer Research Center, Seattle, Washington 98109, ‡‡Department of Biological Sciences, Institute for Bioinformatics and Evolutionary Studies, University of Idaho, Moscow, Idaho 83844, §§Department of Veterinary Integrative Biosciences, Texas A&M University, College Station, Texas 77843, ***Cancer Genetics and Comparative Genomics Branch, National Human Genome Research Institute, National Institutes of Health, Bethesda, Maryland 20892, and †††School of Environment, Griffith University, Nathan, Queensland 4111, Australia

ORCID IDs: 0000-0002-6153-6701 (M.J.M.); 0000-0001-8463-7858 (M.R.-A.); 0000-0001-6075-9738 (E.A.O.)

ABSTRACT Spontaneous tumor regression has been documented in a small proportion of human cancer patients, but the specific mechanisms underlying tumor regression without treatment are not well understood. Tasmanian devils are threatened with extinction from a transmissible cancer due to universal susceptibility and a near 100% case fatality rate. In over 10,000 cases, <20 instances of natural tumor regression have been detected. Previous work in this system has focused on Tasmanian devil genetic variation associated with the regression phenotype. Here, we used comparative and functional genomics to identify tumor genetic variation associated with tumor regression. We show that a single point mutation in the 5′ untranslated region of the putative tumor suppressor *RASL11A* significantly contributes to tumor regression. *RASL11A* was expressed in regressed tumors but silenced in wild-type, nonregressed tumors, consistent with *RASL11A* downregulation in human cancers. Induced *RASL11A* expression significantly reduced tumor cell proliferation *in vitro*. The RAS pathway is frequently altered in human cancers, and *RASL11A* activation may provide a therapeutic treatment option for Tasmanian devils as well as a general mechanism for tumor inhibition.

KEYWORDS cancer; tumor regression; gene expression; tumor suppressor

SPONTANEOUS cancer regression is the reduction or disappearance of a malignant tumor without treatment, and, albeit rare, has been documented in a variety of human cancers (Jessy 2011). Although spontaneous regression has been hypothesized to be associated with exogenous immune stimulation, growth factors, cytokines, and hormonal mediation (Cole 1981; Papac 1998), little is actually known about the underlying mechanisms. Identifying the specific genes and processes driving regression could lead to improved cancer treatments and preventions through targeted immuno- or gene therapies (Mittelman *et al.* 2001; Corrales *et al.* 2015), but ethical considerations prevent the investigation of natural, untreated cancer progression in humans. Therefore, comparative oncological studies in nonhuman systems are needed to identify the mechanisms of important tumor phenotypes such as spontaneous regression.

Recent evidence of spontaneous tumor regression has been documented in natural populations of Tasmanian devils (*Sarcophilus harrisii*) infected with a transmissible cancer (Pye *et al.* 2016a; Wright *et al.* 2017; Margres *et al.* 2018). Although most cancers are somatic in origin, Tasmanian devils are threatened with extinction by the emergence and rapid spread of two, independently derived, transmissible cancers

doi: https://doi.org/10.1534/genetics.120.303428
Manuscript received May 5, 2020; accepted for publication June 12, 2020; published Early Online June 18, 2020.
Supplemental material available at figshare: https://doi.org/10.25386/genetics.12498896.
[1]Corresponding author: Harvard University, 52 Oxford St., Cambridge, MA. E-mail: mark_margres@fas.harvard.edu

[devil facial tumor disease (DFTD) and DFT2] (Murchison *et al.* 2012; Pye *et al.* 2016b; Stammnitz *et al.* 2018; Storfer *et al.* 2018). DFTD and DFT2 are contagious tumor cell lines spread via biting during common social interactions (Hamede *et al.* 2013), and both tumors have nearly a 100% case fatality rate. Although DFT2 was discovered only recently in 2014, and has so far remained limited in its geographic spread (Pye *et al.* 2016b; Stammnitz *et al.* 2018), DFTD has spread across ∼95% of the devil's geographic range and has caused localized declines >90% over the last 23 years (McCallum 2008). Several Tasmanian devils with confirmed DFTD in northwestern Tasmania, however, were recently recaptured with either substantial tumor shrinkage or entire disappearance of the tumor (Figure 1 and File S1; Pye *et al.* 2016a; Wright *et al.* 2017; Margres *et al.* 2018).

Similar to the focus on patient immunological responses to human cancers (Morgan *et al.* 2006; Sharma *et al.* 2017), recent studies have focused on Tasmanian devil genetic variation associated with DFTD regression and found putative regulatory variation in candidate genes associated with angiogenesis and cancer risk (Wright *et al.* 2017; Margres *et al.* 2018). DFTD-specific mechanisms, however, have not yet been investigated, and tumor genetic variation can affect oncogenicity (Bailey *et al.* 2018). Here, we build on our previous work in the hosts (Margres *et al.* 2018), and used comparative and functional genomics to identify tumor-intrinsic factors associated with spontaneous regression in the matching DFTD samples (*i.e.*, matched tumor-normal design). We compared regressed and nonregressed tumor genomes and transcriptomes and found a single point mutation that activated the tumor suppressor gene *RASL11A* in regressed tumors. We then used *in vitro* cell proliferation assays to show that tumor cell proliferation was significantly inhibited by virally induced *RASL11A* expression in three of four tumor cell lines. Taken together, our results suggest that *RASL11A* activation may be a general mechanism for tumor inhibition.

Materials and Methods

DFTD sampling

Tasmanian devils were trapped in northwestern Tasmania using custom-built traps as previously described (Figure 1; Hamede *et al.* 2015). Following capture, devils were tagged with microchip transponders (Allflex NZ Ltd, Palmerstone North, New Zealand), aged, inspected for DFTD, and released; DFTD status was determined by histopathological confirmation of tumor biopsies, and tumor volume was measured for all infected individuals. To confidently assign a phenotypic designation to a tumor (*i.e.*, regressed or nonregressed), we required tumors to be sampled at multiple time points. Tumors were classified as regressed if total tumor volume decreased ≥15% of the initial tumor volume upon recapture for Tasmanian devils previously confirmed to be infected with DFTD as described elsewhere (Margres *et al.* 2018). Otherwise, tumors were classified as nonregressed (Figure 1). One exception to these criteria was Nonregressed 1. Although this tumor was only sampled a single time-point, the individual host was disease free in 2012, retrapped in 2013 with DFTD, was in extremely poor body condition, and ultimately euthanized by the Save the Tasmanian Devil Program; moribund animals such as this have never been shown to recover. Given the sample size limitations of this study, we were confident in the classification of this tumor as nonregressed due to its rapid growth and clear negative consequences on host health. Raw tumor volume data are provided in Supplemental Material, File S1. Animal use was approved by the IACUC at Washington State University (#04392; ASAF), the University of Tasmania Animal Ethics Committee (A0008588, A0010296, A0011696, A0013326, A0015835), and the Department of Primary Industries, Parks, Water and Environment Animal Ethics Committee. Demographic information for the matching hosts samples can be found in Margres *et al.* (2018).

Whole-genome sequencing

We performed initial whole-genome sequencing for 12 DFTD tumors; these tumors were collected from 11 Tasmanian devils in northwestern Tasmania as previously described (Margres *et al.* 2018). Eight tumors exhibited tumor regression (Regressed 1–8; Figure 1) and four tumors did not (Nonregressed 1–4; Figure 1). Three regressed tumors (Regressed1, 3, and 6; Figure 1 and Figure S1) were serially sampled several months apart and resequenced (*i.e.*, we sequenced 15 total genomes across 12 individual tumors). Genomic DNA was extracted from tumor biopsies. Whole genomes for each tumor were sequenced 150 PE on an Illumina HiSeq X platform to ∼90× coverage. Sequencing was performed at the Northwest Genomics Center at the University of Washington (Seattle, WA) and GENEWIZ (South Plainfield, NJ).

Alignments and variant calling

We merged and trimmed reads with FLASH2 (Magoč and Salzberg 2011) and Sickle (Joshi and Fass 2011), respectively. Merged and unmerged reads were aligned to the Tasmanian devil reference genome (downloaded from Ensembl January 2016; Murchison *et al.* 2012) using the BWA-MEM algorithm (Li and Durbin 2009). We identified ∼2.6 million SNPs using HaplotypeCaller in GATK (McKenna *et al.* 2010; DePristo *et al.* 2011) as previously described (Margres *et al.* 2017). To identify somatic or cancer-specific SNPs, we performed a hard filter and removed any SNP previously identified in the paired host (*i.e.*, Tasmanian devil) samples from Margres *et al.* (2018). We identified ∼1.4 million somatic SNPs across all 15 initial genomes (12 individual tumors) following the hard filter. These variants were then filtered in VCFtools (Danecek *et al.* 2011) and were required to possess a minimum depth value of 15 and a minimum genotype quality of 60 as previously described (Margres *et al.* 2018). We identified 632,756 somatic variants that passed filter across the 15 tumor genomes.

Identifying the genomic basis of tumor regression

We used the Genotype Phenotype Association Toolkit (GPAT++) from the vcflib package (Garrison 2012) as previously described (Domyan *et al.* 2016) to identify genomic differentiation between regressed and nonregressed tumors. Differentiation was identified using the pFst function. pFst uses a likelihood ratio test to identify allele frequency differences across groups while simultaneously accounting for potential sequencing error. We calculated pFst values for 471,676 SNPs when comparing the eight regressed and four nonregressed tumors (Nonregressed 1–4; Figure 1). For these comparisons, only the initial sample was used for the three regressed tumors (Regressed 1a, 3a, and 6a; Figure 1 and Figure S1) that were sequenced multiple times. SNPs were identified as candidate variants if they occurred in the top 0.1% ($P \leq 0.0137$) of the most differentiated SNPs. These candidates were characterized using variant effect predictor (VEP; McLaren *et al.* 2016) and the Tasmanian devil reference genome (downloaded from Ensembl January 2016; Murchison *et al.* 2012). Only nonsynonymous variants or variants in untranslated regions (UTRs) were functionally investigated in the current study because these variants were (1) most likely to affect the regression phenotype in a tractable manner, and (2) could be functionally validated (see below). We used GeneCards (www.genecards.org; Stelzer *et al.* 2016) to identify putative gene function.

Tumor phylogenetics

We took two approaches to infer unrooted tumor phylogenies for Regressed 1–8 and Nonregressed 1–4 tumors (Figure 1). First, we followed the approach of Margres *et al.* (2019) and used SVDquartets (Chifman and Kubatko 2014) in PAUP* v4.0a157 (Swofford 1998) to infer an unrooted phylogeny based on the filtered, somatic SNP data described above. We used PGDspider v2.1.1.2 (Lischer and Excoffier 2012) and custom scripts to produce multiple sequence alignments in fasta format, and concatenated the two alignments generated for each individual tumor. All quartets were estimated under the multispecies coalescent model (expecting matrix-rank 10), and these quartets were assembled using the QFM algorithm. Confidence in tree topology was estimated using nonparametric bootstrapping. We used the SumTrees program in DendroPy v4.3.0 (Sukumaran and Holder 2010) to summarize across bootstrapped trees and produce the consensus tree (Margres *et al.* 2019). The consensus tree was visualized in FigTree v1.4.3 (Rambaut 2012). Second, we used RAxML v8 (Stamatakis 2014) on the CIPRES Science Gateway (Miller *et al.* 2010). Briefly, we conducted rapid bootstrapping (100 replicates) and searched for the highest-scoring ML tree. Because we were using exclusively SNP data, we performed an ascertainment bias correction to correct branch-length estimates (Leaché *et al.* 2015). To accomplish this, RAxML was run using the following parameter settings: -f a, -m ASC_GTRCAT, -j –HKY85, -c 4, -N 100, –asc-corr felsenstein. As with the SVDquartets phylogeny, the RAxML ML tree was visualized using FigTree (Rambaut 2012), with bootstrap nodal support values shown.

Additional nonregressed tumor sequencing and analysis

We recognize that nonregressed tumors may appear to be easy to access given the higher frequency of the phenotype (*i.e.*, wild type) in the population, but sampling confirmed nonregressed tumors was challenging. To confidently assign a phenotypic designation to a tumor (*i.e.*, regressed or nonregressed), we required tumors to be sampled at multiple time points as described above. Given that devils infected with wild-type, nonregressing tumors ultimately perish faster than devils with regressed tumors, recapture following infection (and therefore confirmation of the nonregressing phenotype) was not as frequent as one might expect. Following our initial round of sequencing, we were able to sample three additional nonregressed tumor samples from the same geographic region (Nonregressed 5–7; Figure 1), and these three tumors represent all tumors that we could confirm (with some degree of confidence) as nonregressed. To confirm the candidate genotypes identified from the analyses above, we performed a second round of whole-genome sequencing for the three additional nonregressed DFTD tumors (Nonregressed 5–7; Figure 1). DNA was extracted from tumor biopsies and libraries were prepped using the NEBNext Ultra II DNA Library Prep Kit for Illumina (New England BioLabs, product E7645S). Whole-genomes for each tumor were sequenced 150 PE on an Illumina HiSeq X platform to $\sim$20$\times$ coverage at the Northwest Genomics Center at the University of Washington (Seattle, WA). We again merged and trimmed reads with FLASH2 (Magoč and Salzberg 2011) and Sickle (Joshi and Fass 2011), respectively. Merged and unmerged reads were again aligned to the Tasmanian devil reference genome (downloaded from Ensembl January 2016; Murchison *et al.* 2012) using the BWA-MEM algorithm (Li and Durbin 2009). SNPs were identified using HaplotypeCaller in GATK (McKenna *et al.* 2010; DePristo *et al.* 2011) with the following criteria: mean depth of 8, meanQ of 60, and maf of 0.05.

Tumor transcriptomics

RNA was extracted from two regressed and two nonregressed tumor biopsies using a standard Trizol method as previously described (McGivern *et al.* 2014). Of the four samples sequenced, one regressed (Regressed 1a) and one nonregressed (Nonregressed 2) tumor were included in the genome sequencing described above; the other two samples were not previously sequenced. Tissues were not available for the remaining samples, and because regression is such a rare phenotype, only one additional regressed sample (*i.e.*, the additional transcriptome sample sequenced here) was collected during the course of the study. Sequencing and cDNA library preparation were performed by the Genomics Core at Washington State University, Spokane (Spokane, WA). Each library was sequenced 100 PE across four lanes of an Illumina HiSeq 2500, and each transcriptome had

29.2–30.3 million reads. Low quality bases were trimmed with Trim Galore! version 0.4.5, and transcriptomes were assembled using the "new Tuxedo" package (Pertea *et al.* 2016). Here, reads were aligned to the reference genome (downloaded from Ensembl January 2016; Murchison *et al.* 2012) using HiSat2 version 2.1.0 (Kim *et al.* 2015), transcripts assembled and expression quantified using StringTie version 1.3.4 (Pertea *et al.* 2015), and analyzed/visualized in Ballgown (Fu *et al.* 2018). Alignment rates were >91% for all samples.

Lentiviral vector gene delivery

Four tumor cell lines (three DFTD lines and one DFT2 line) and a Tasmanian devil fibroblast cell line (Murchison *et al.* 2012) were grown in RPMI 640 media supplemented with 10% fetal bovine serum and penicillin/streptomycin. The Tasmanian devil fibroblast cell line was described elsewhere (Murchison *et al.* 2012). DFTD-a (DFT1-10181), DFTD-b (DFT1-A48), and DFTD-c (DFT1-c5065) were derived from primary DFTD tumors collected from Low Head, Tasmania in 2014, Bronte Park, Tasmania in 2004, and Bangor, Tasmania in 2007, respectively. The DFT2 cell line (DFT2-Jarvis) was derived from a primary DFT2 tumor collected from Nicholls Rivulet, Tasmania in 2015.

For each of the five cell lines described above, the Tasmanian devil *RASL11A* coding-sequence was cloned into a pCIG vector containing the puromycin N-acetyltransferase gene in place of enhanced green fluorescent protein (eGFP). A *RASL11A* gBlock was synthesized and inserted into the multiple cloning site of pCIG by Gibson assembly (Gibson *et al.* 2009). The pCIG *RASL11A* plasmid was digested with *Age*I and *Mlu*I to remove eGFP. Puro was PCR amplified from GIPZ vector and ligated to the pCIG plasmid backbone to generate pCI puro-*RASL11A*. The eGFP lines did not express *RASL11A* and were considered control lines, and the pCI or *RASL11A* lines expressed *RASL11A* and were considered our case lines (see below; Figure S2 and File S2).

Real-time qPCR assays

Cellular RNA was extracted from 10 cm^2 of tissue culture by guanidinium thiocyanate-phenol-chloroform extract. RNA (1 μg) was converted to cDNA using iScript Reverse Transcription Supermix for RT-qPCR (Bio-Rad) according to the manufacturer's protocol. Real-time qPCR assays were conducted on the QuantStudio for *RASL11A* (forward: 5′–TCCCATTCCGGAG TCTTCCT–3′; reverse: 5′–CCTCTGCCCACTGAACACAT–3′) and *RPS29* (forward: 5′–ATGGGTCATCAGCTCTAC–3′; reverse: 5′–AGGCCGTATTTGCGGATTAG–3′). Relative changes in expression were analyzed using the $2^{-\Delta\Delta C_T}$ method (Livak and Schmittgen 2001) where the relative expression level for the locus of interest (*i.e.*, *RASL11A*) was compared to the expression level of the house-keeping gene *RPS29* (File S2). We used paired, one-tailed *t*-tests to compare mean expression levels for *RASL11A* (Figure S2) across individual case-control assays for each cell line. Each assay included two to three replicates per cell line.

Cell proliferation assays

For each cell line described above, 3000 cells per well were seeded in 96-well flat bottom culture plates in RPMI 1640 medium supplemented with 10% fetal bovine serum and penicillin/streptomycin. Cell Titer-Glo assays were performed in triplicate. Cell Titer-Glo assays quantify the amount of ATP present, a proxy for the number of metabolically active cells and cell proliferation. ATP was quantified at days 0, 3, 4, 6, 7, and/or 11 according to the manufacturer's protocol. In total, we performed five assays (18 total replicates) for the Tasmanian devil fibroblast line and five (17 total replicates), five (18 total replicates), two (7 total replicates), and two (7 total replicates) assays for the DFTD-a, DFTD-b, DFTD-c, and DFT2 tumor lines, respectively (File S2).

To determine if *RASL11A* expression reduced tumor cell proliferation significantly more often than expected by chance, we used a χ^2 test to compare the observed frequency of replicates where the *RASL11A* line had a lower, final viable cell count than the control line *vs.* the expected frequency. If *RASL11A* expression did not affect tumor cell proliferation, we would expect the *RASL11A* lines to exhibit a greater proliferation rate than the control line (and vice versa) in ∼50% of the replicates (*i.e.*, our expected frequencies). We performed this test across all 49 tumor replicates as well as for DFTD and DFT2 independently. To visualize the cell proliferation assay results in Figure 3, we calculated the relative proliferation rate for the *RASL11A* line as the ratio of the *RASL11A* line ATP luminescence estimate to the control line ATP luminescence estimate (*i.e.*, case/control). Ratios >1 represent increased proliferation under *RASL11A* expression whereas ratios <1 represent decreased proliferation under *RASL11A* expression. We calculated these ratios for all replicates across all timepoints. One-sample *t*-tests were used to determine whether the final mean relative proliferation estimates significantly differed from one where a ratio of one represents the null expectation of identical proliferation between *RASL11A* and control lines.

Data availability

The authors state that all data necessary for confirming the conclusions presented in the article are represented fully within the article. All raw sequencing data were deposited in the Sequence Read Archive (SRA) under BioProject PRJNA472767. Whole-genome raw reads are under accessions SRR7257499–SRR7257513 and SRR10436678, 79, and 81. Transcriptome raw reads are under accessions SRR7257322–SRR7257325. Raw functional genomic data are provided in File S2. Supplemental material available at figshare: https://doi.org/10.25386/genetics.12498896.

Results

Comparative genomics of regressed and nonregressed tumors

To identify putative causal mutations underlying spontaneous tumor regression in DFTD, we sequenced the genomes of four

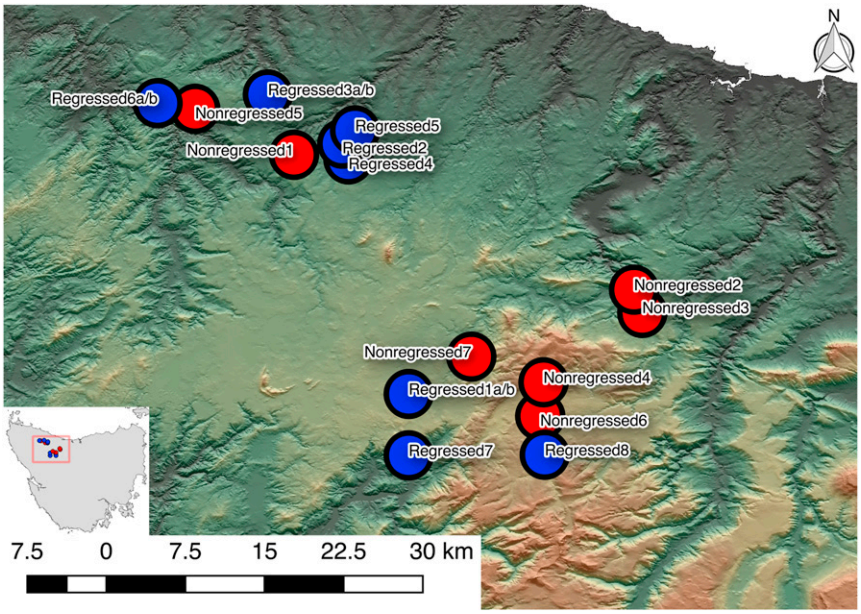

Figure 1 Sampling of Devil Facial Tumor Disease. We collected tissue samples from 15 tumors for whole-genome sequencing from northwest Tasmania (see inset). Eight of these tumors underwent tumor regression ("Regressed" shown in blue) whereas the other seven did not ("Nonregressed" shown in red). Regressed 1, Regressed 3, and Regressed 6 were serially sampled, and timepoints are indicated as (a) and (b), respectively. Nonregressed 1–4 were included in initial analyses, and nonregressed 5–7 were sequenced following these initial analyses to increase sample size. See File S1 for additional data.

nonregressed (Nonregressed 1–4) and eight regressed tumors (Regressed 1–8; Figure 1); the latter represent all available tumors that exhibited ≥ 15% reductions in tumor volume following recapture of the infected Tasmanian devil, with several cases of complete tumor clearance (Figure 2B and File S1; Margres *et al.* 2018). We identified 471,676 tumor-specific SNPs across the 12 tumor genomes, similar to previous analyses that identified 691–699 k SNPs across two DFTD genomes (Murchison *et al.* 2012); none of these variants were identified in the genomes of the Tasmanian devils that possessed the tumors examined in this study (Margres *et al.* 2018). Because most discovered variants were intergenic (∼75%), SNPs were identified as candidates if they were highly differentiated (*i.e.*, top 0.1% of most differentiated somatic variants; $P \leq 0.0137$) and resulted in nonsynonymous substitutions or occurred in putative regulatory regions. We did not identify any candidate nonsynonymous SNPs, consistent with previous work showing a general paucity of nonsynonymous variation among DFTD (Stammnitz *et al.* 2018). We did, however, identify two candidate variants in the 5′ untranslated regions (UTRs) of *RASL11A* and *ERICH6* ($P = 0.0105$; Figure 2A). Both candidates involved T↔C transitions, the most common mutation in human cancers (Bailey *et al.* 2018). For each locus, we identified a near fixed genotypic difference (Figure 2C). All four nonregressed tumors were homozygous for the reference allele (T/T for *RASL11A* and C/C for *ERICH6*). Six of the seven genotyped regressed tumors were heterozygous at each site (T/C); one regressed tumor (Regressed 8) was not genotyped due to missing data. The only regressed tumor that was not heterozygous at either locus (Regressed 3 in Figure 2C) represented a unique case where an individual Tasmanian devil possessed both regressed (Regressed 3) and nonregressed (Nonregressed 3) tumors. These tumors were sister to one another in one of our two phylogenetic analyses (Figure S1), suggesting potential metastasis and within host tumor divergence. Here, regression may be a product of host genetic variation (Margres *et al.* 2018) and/or immune response (see *Discussion*; Pye *et al.* 2016a).

To increase the nonregressed tumor sample size, we sequenced an additional three nonregressed tumor genomes at lower coverage and genotyped each sample at both the *RASL11A* and *ERICH6* candidate sites (Nonregressed 5–7 in Figure 1 and File S1). For each candidate variant, two of the three nonregressed tumors were homozygous for the reference allele, but one nonregressed tumor was heterozygous at both sites. Overall, six of seven nonregressed tumors were homozygous and six of seven regressed tumors were heterozygous at each allele. The near fixed genotypic differences in putative regulatory regions for *RASL11A* and *ERICH6* suggested that expression variation at either locus may contribute to tumor regression. Although the function of *ERICH6* is not known, *RASL11A* is a regulator of rDNA transcription and a putative tumor suppressor (Pistoni *et al.* 2010). *RASL11A* expression is downregulated in human prostate tumors (Louro *et al.* 2004) and hypermethylated in colon cancer cell lines (Weber *et al.* 2005), suggesting that *RASL11A* expression may negatively affect oncogenicity.

RASL11A expression associates with tumor regression

To determine if these UTR variants affected the expression of either candidate gene, we sequenced the transcriptomes for two regressed and two nonregressed tumors (tissues were not available for remaining samples). *ERICH6* was not assembled in any of the four transcriptomes, indicating its lack of expression in either tumor type. *RASL11A* was expressed

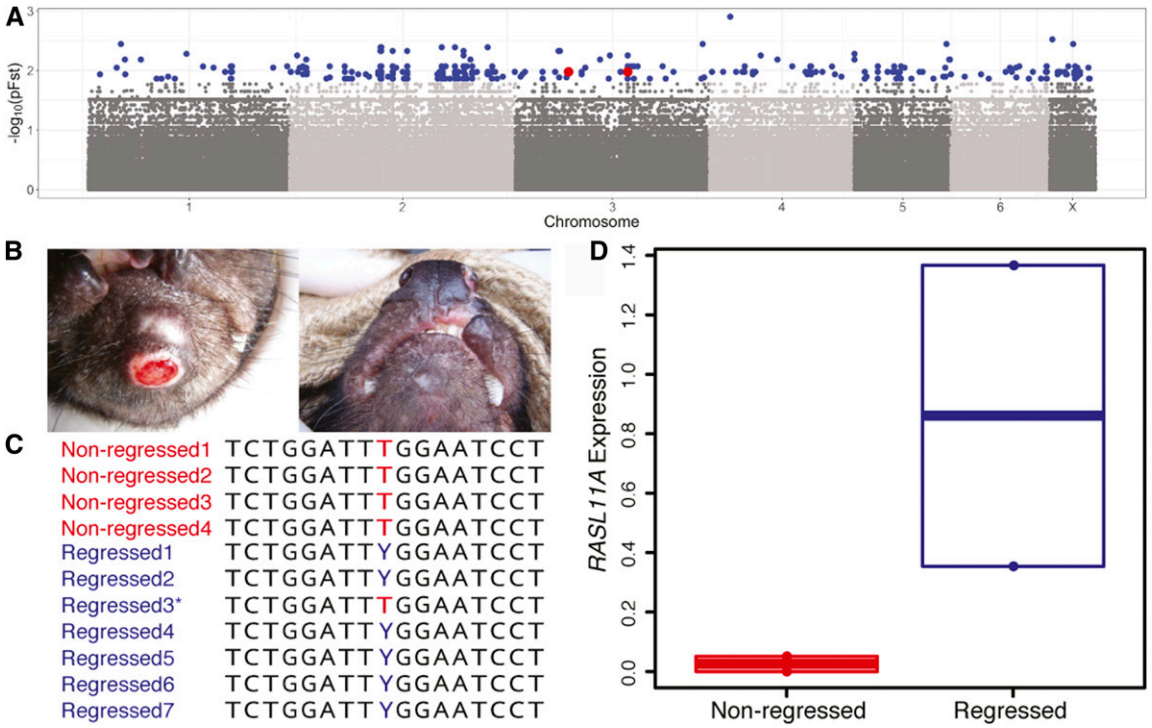

Figure 2 Genetic differentiation underlying tumor regression in Devil Facial Tumor Disease. (A) Manhattan plot showing genetic differentiation between regressed (n = 8) and nonregressed (n = 4) tumors. Blue points represent the most differentiated SNPs (top 0.1% of the empirical pFst distribution; $P \leq 0.0137$). SNPs were considered candidates if they were nonsynonymous or occurred in a putative regulatory region. Red points represent the two candidates identified in the 5′ untranslated regions (UTRs) of *RASL11A* and *ERICH6* (P = 0.0105). The x-axis represents genomic position using the Tasmanian devil reference genome. The y-axis represents the negative log of the pFst statistic with genetic differentiation increasing along the axis. (B), Photos of a regressed tumor found in an adult female Tasmanian devil. Photo on the left was taken in August 2011. Photo on the right was taken in May 2012. *Photo credit*: Rodrigo Hamede. (C), Alignment of the 5′ UTR of *RASL11A*. Both *ERICH6* and *RASL11A* showed a near fixed genotypic difference at the candidate sites; only *RASL11A* is shown here. All four nonregressed tumors were homozygous reference, and six of the seven genotyped regressed tumors were heterozygous (represented by Y). The only regressed tumor that was not heterozygous at either locus (Regressed 3, indicated with an * above) was a unique case where a single Tasmanian devil possessed both regressed (Regressed 3) and nonregressed (Nonregressed 3) tumors. One regressed tumor (Regressed 8) was not genotyped at either site due to missing data. (D), *RASL11A* expression in regressed (n = 2) and nonregressed (n = 2) tumor transcriptomes. *RASL11A* was differentially expressed, although the trend was not significant due to sample size limitations (P = 0.0769). The y-axis represents $\log_2 FPKM + 1$. *ERICH6* was not expressed in any transcriptome.

in regressed tumors but was not expressed in nonregressed (*i.e.*, wild-type) tumors (Figure 2D), consistent with its putative role as a tumor suppressor and underexpression in human prostate cancer and colon cancer cell lines (Louro *et al.* 2004; Weber *et al.* 2005). Transcriptome sequence data confirmed the expression of the *RASL11A* regressed allele in both regressed tumor samples (one of which was not sequenced above; see "*Materials and Methods*" for details), suggesting that the candidate variant in the 5′ UTR of *RASL11A* may have led to the expression of this tumor suppressor in regressed tumors, and, ultimately, tumor regression.

In vitro assays confirm RASL11A expression reduces tumor cell proliferation

To directly test whether *RASL11A* expression negatively affected tumor cell proliferation or survival, we used lentiviral vector gene delivery to create cell lines that expressed *RASL11A* (*i.e.*, case lines) and those that did not (*i.e.*, eGFP control lines) across four tumor cell lines (three DFTD lines and one DFT2 line) and a Tasmanian devil fibroblast cell line. *RASL11A* delivery was confirmed using qPCR (see Figure S2). We then measured cell proliferation and survival for all cell lines (7–18 replicates/line; see "*Materials and Methods*" and File S2). To determine if *RASL11A* expression reduced tumor proliferation significantly more often than expected by chance, we used a χ^2 test to compare the observed frequency of replicates where the *RASL11A* line had a lower, final viable cell count than the control line *vs.* the expected frequency (*i.e.*, equal frequencies; see "*Materials and Methods*" for details). We found that *RASL11A* expression decreased overall cell proliferation in the tumor lines significantly more frequently than expected by chance (39/49 replicates; χ^2 = 17.163, df = 1, $P < 0.0001$; File S2); DFTD lines (32/42 replicates; χ^2 = 11.524, df = 1, P = 0.0007) and the DFT2 line (7/7 replicates; χ^2 = 7.000, df = 1, P = 0.0082) remained significant when analyzed independently. Conversely, *RASL11A* expression significantly increased cell proliferation in Tasmanian devil fibroblasts more frequently than expected by chance (17/18 replicates; χ^2 = 14.222,

df = 1, *P* = 0.0002; File S2). These discordant effects of *RASL11A* expression on cell proliferation across host and tumor cell lines were not surprising as genes can often function in opposite directions across different cell types, especially cancer (Vogelstein *et al.* 2013).

We next calculated *RASL11A* line relative proliferation (*RASL11A* line proliferation/control line proliferation) for each replicate across all cell lines. Here, ratios <1 indicated reduced proliferation under *RASL11A* expression, ratios >1 indicated increased proliferation under *RASL11A* expression, and ratios ~1, the null hypothesis, represented equal proliferation across *RASL11A* and control lines. *RASL11A* expression significantly reduced cell proliferation in three of the four tumor cell lines ($0.0001 \leq P \leq 0.0256$); DFTD-b did not show a significant difference across the *RASL11A* and control lines ($P = 0.0783$). *RASL11A* expression significantly increased cell proliferation in Tasmanian devil fibroblasts ($P = 0.0287$; Figure 3), as expected. Here, the DFTD-b line may have adapted to the culture environment (*e.g.*, compensatory mutation may have restored tumor growth rates in the *RASL11A*+ line). We also cannot rule out the role of host response (Pye *et al.* 2016a; Margres *et al.* 2018) or other factors independent of *RASL11A* expression that may have contributed to spontaneous tumor regression. Nonetheless, our results suggest an important, but not exclusive, role of *RASL11A* expression in tumor regression.

Discussion

We present several lines of evidence that *RASL11A* contributes to spontaneous, natural tumor regression. First, we used whole-genome sequencing to identify a near fixed genotypic difference between regressed and nonregressed tumors in a putative regulatory region for the tumor suppressor gene *RASL11A*. Second, we used transcriptomics, albeit in a few samples, to demonstrate that *RASL11A* was silenced in wild-type, nonregressed tumors but activated in regressed tumors, consistent with the genotypic data as well as *RASL11A* expression in human prostate (Louro *et al.* 2004) and colon (Weber *et al.* 2005) cancers. Third, we used cell proliferation assays to show that *RASL11A* activation significantly and negatively affected cancer cell proliferation *in vitro* in three of the four tumor cell lines investigated. Although we sequenced all confirmed cases of tumor regression at the time of the study, we recognized the limitations our sample size placed on interpreting the genomic and transcriptomic analyses. Therefore, by using functional genomics to show that *RASL11A* expression significantly impeded tumor cell proliferation *in vitro* across multiple, independent cell lines representing two independent transmissible cancers (DFTD and DFT2), our results collectively indicated that spontaneous cancer remission in Tasmanian devils is mediated, in part, by the expression of the tumor suppressor *RASL11A*.

The evolutionary implications of the *RASL11A* allele/regression phenotype are still largely unclear. Trade-offs between pathogen transmission and virulence have been widely discussed [*e.g.*, reviewed in Cressler *et al.* (2016)], and successful transmission at the population level is directly related to the specific physiological interactions occurring within a single host. The *RASL11A* allele could be beneficial to DFTD fitness by increasing the duration of infection and opportunity for transmission (*i.e.*, reduced virulence leads to greater

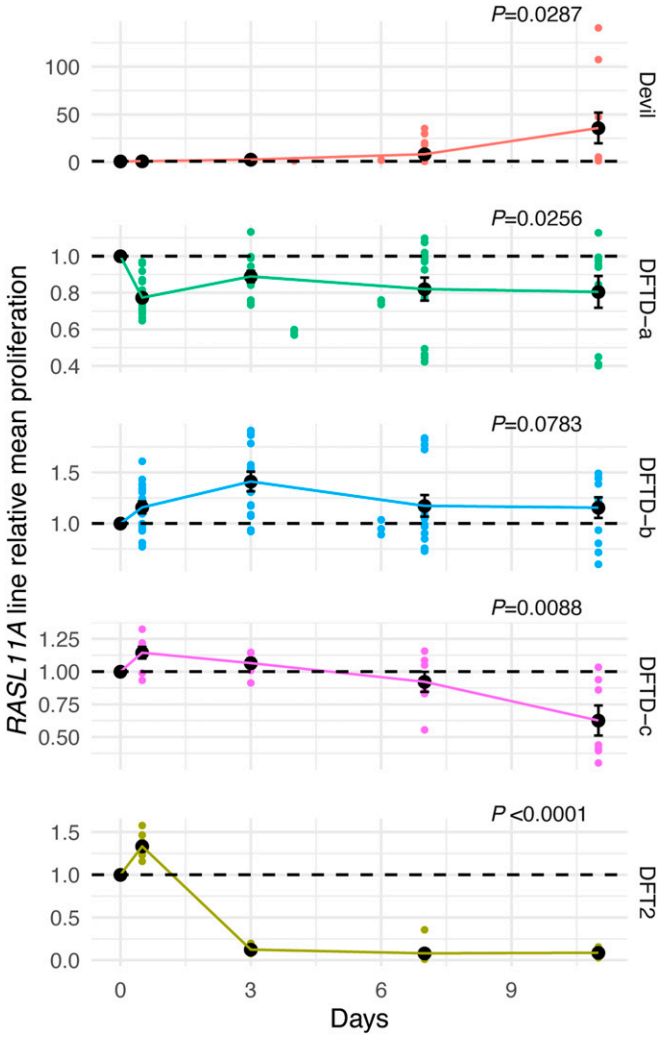

Figure 3 *RASL11A* expression reduced tumor cell proliferation *in vitro*. Cell Titer-Glo assays were used to estimate the amount of ATP present, a proxy for the amount of metabolically active cells and cell proliferation, for control (− *RASL11A* expression) and *RASL11A* (+*RASL11A* expression) lines for the five cells lines in culture: Tasmanian devil fibroblast line (Devil), three DFTD lines (DFTD-a–c), and one DFT2 line. ATP was quantified at days 0.5, 3, 4, 6, 7, and/or 11. Means were estimated for days 0, 0.5, 3, 7, and 11. Relative proliferation was calculated as the ratio of *RASL11A* line ATP levels to control line ATP levels for each replicate at each timepoint and is shown on the *y*-axis. Ratios <1 indicate reduced proliferation under *RASL11A* expression, ratios >1 indicate increased proliferation under *RASL11A* expression, and ratios =1 (represented by the horizontal dashed line) represent equal proliferation across *RASL11A* and control lines. Colored points represent individual replicates, black points represent the mean estimate across all replicates for that time point, and error bars represent the SE. *P*-values were calculated using a one-sample *t*-test to determine if final relative mean proliferation significantly differed from one (*i.e.*, the null hypothesis that proliferation would be equivalent across *RASL11A* and control lines).

transmission), deleterious to DFTD fitness by reducing growth and, therefore, transmission rates, or the result of stochastic, neutral processes and not subjected to strong selective pressures. Additional geographic and temporal sampling are needed to truly understand (1) how *RASL11A*-mediated tumor regression will affect Tasmanian devil and DFTD evolution, and perhaps coevolution, going forward, and (2) whether the *RASL11A* allele/regression phenotype arose independently multiple times or a single time; our unrooted phylogenies (Figure S1) and limited sampling were unable to address these questions.

Although transmissible cancers are rare, with the only natural occurrences found in dogs [canine transmissible venereal tumor (CTVT; Murgia *et al.* 2006), bivalves (Metzger *et al.* 2016), and Tasmanian devils (Pearse and Swift 2006; Pye *et al.* 2016b], CTVT has also been shown to naturally regress. Here, the tumor grows progressively (P-phase) prior to spontaneous regression (R-phase), and this regression has been hypothesized to be the result of reduced tumor cell proliferation (Chu *et al.* 2001), similar to our results. More recent work examined vincristine-mediated CTVT regression and found that, following treatment, regression occurred in sequential steps involving immune system activation and infiltration of the tumor (Frampton *et al.* 2018). Although this work focused on tumor regression following vincristine treatment, host innate immunity certainly can play an important role in triggering cancer regression. Indeed, previous work on DFTD has also shown evidence of host immune response associating with spontaneous regression (Pye *et al.* 2016a). T lymphocyte infiltration, serum antibodies, and other immune responses could explain (among other factors) why the *RASL11A* allele was not fixed in regressed tumors. For each special case where the *RASL11A* allele did (Nonregressed 7) and did not (Regressed 3) lead to regression as expected, host immune response (Pye *et al.* 2016a), host genetic variation (Margres *et al.* 2018), and/or other factors may explain the discordant patterns. For example, Regressed 3 was the only regressed tumor in our study that was not heterozygous at the *RASL11A* allele. Regressed 3 was sampled from a Tasmanian devil that also possessed a nonregressed tumor (Nonregressed 3), and these tumors were sister to one another in one of our two phylogenetic analyses (Figure S1). Here, regression may be a product of serum antibody development following initial exposure to Nonregressed 3, with regression in the second tumor (*i.e.*, Regressed 3) being the product of host immune response following metastasis (Pye *et al.* 2016a). Additional immunological and histological work is needed to assess the relative roles host immunity, host genetics, and tumor genetics each play in relation to spontaneous tumor regression as *RASL11A* expression cannot universally be the sole driver of regression.

Although tumor regression in DFTD, like many tumor phenotypes, may have a polygenic basis (*e.g.*, ERBB inhibition was recently shown to also arrest DFTD cell growth *in vitro*; Kosack *et al.* 2019), interference with a single mutant gene product can be sufficient to arrest cancer growth (Vogelstein *et al.* 2013). Indeed, a recent meta-analysis in human cancers found that one mutation is sufficient to affect RAS pathway function (Sanchez-Vega *et al.* 2018), and mutated RAS alleles are found in ∼30% of all human cancers (Bos 1989; Way *et al.* 2018). *RASL11A* is underexpressed in human prostate cancer relative to normal prostate tissue (Louro *et al.* 2004) and is highly methylated (and not expressed) in colon cancer cell lines (Weber *et al.* 2005). Other than one recent study that found that *RASL11A* was also underexpressed in colorectal cancer (although *RASL11A* activation did not impede cancer growth *in vitro*; Wangsa *et al.* 2019), *RASL11A* function has been relatively unexplored. *RASL11A* is a known positive regulator of RNA polymerase I transcription and modulator of pre-rRNA synthesis (Pistoni *et al.* 2010), suggesting that the mechanism by which *RASL11A* inhibits DFTD growth may be through the dysregulation of rRNA transcription and processing. rRNA transcription is critical to cellular metabolism and ribosome biosynthesis, and misregulation of this process is a recurrent motif in human cancer due to the increased metabolic demands of uncontrolled cell growth (Roche *et al.* 2017). As such, rRNA synthesis is a key target in human cancer therapeutics (Drygin *et al.* 2009), and *RASL11A* activation may provide a therapeutic treatment option for Tasmanian devils as well as a mechanism for tumor inhibition in certain human cancers.

Spontaneous tumor regression in human cancers only occurs in ∼1 of 60,000−100,000 cases (∼0.001%; Missotten *et al.* 2008; Sengupta *et al.* 2010). Ethical considerations prevent the investigation of natural, untreated cancer progression in humans, highlighting the need for comparative oncological studies in nonhuman systems to identify the mechanisms underlying important tumor phenotypes such as spontaneous regression. Our findings in a system without therapeutic intervention and across two independently derived cancers highlight the relevance of *RASL11A* activation as a natural mechanism of tumor inhibition and a potential target in cancer therapy.

Acknowledgments

This work was funded by National Institutes of Health (NIH) grant R01-GM126563-01 and National Science Foundation (NSF) grant DEB 1316549 to A.S., P.A.H., H.M., and M.E.J. as part of the joint NIH-NSF-United States Department of Agriculture (USDA) Ecology and Evolution of Infectious Diseases program, the Australian Research Council (ARC) Future Fellowship (FT100100250) to M.J., ARC Large Grants (A00000162) to M.J., Linkage (LP0561120) to M.J. and H.M., Discovery (DP110102656) to M.J. and H.M., and DECRA (170101116) to R.H. Additional support was provided by the Sarah and Daniel Hrdy Fellowship at Harvard University to M.J.M. Additional support was also provided by NIH P30 GM103324.

Literature Cited

Bailey, M., C. Tokheim, E. Porta-Pardo, S. Sengupta, D. Bertrand *et al.*, 2018 Comprehensive characterization of cancer driver genes and mutations. Cell 173: 371–385.e18. https://doi.org/10.1016/j.cell.2018.02.060

Bos, J., 1989 Ras oncogenes in human cancer: a review. Cancer Res. 49: 4682–4689.

Chifman, J., and L. Kubatko, 2014 Quartet inference from SNP data under the coalescent. Bioinformatics 30: 3317–3324. https://doi.org/10.1093/bioinformatics/btu530

Chu, R., C. Lin, C. Liu, S. Yang, Y. Hsiao *et al.*, 2001 Proliferation characteristics of canine transmissible venereal tumor. Anticancer Res. 21: 4017–4024.

Cole, W., 1981 Efforts to explain spontaneous regression of cancer. J. Surg. Oncol. 17: 201–209. https://doi.org/10.1002/jso.2930170302

Corrales, L., L. Glickman, S. McWhirter, D. Kanne, K. Sivick *et al.*, 2015 Direct activation of STING in the tumor microenvironment leads to potent and systemic tumor regression and immunity. Cell Rep. 11: 1018–1030. https://doi.org/10.1016/j.celrep.2015.04.031

Cressler, C., D. McLeod, C. Rozins, J. Van Den Hoogen, and T. Day, 2016 The adaptive evolution of virulence: a review of theoretical predictions and empirical tests. Parasitology 143: 915–930. https://doi.org/10.1017/S003118201500092X

Danecek, P., A. Auton, G. Abecasis, C. Albers, E. Banks *et al.*, 2011 The variant call format and VCFtools. Bioinformatics 27: 2156–2158. https://doi.org/10.1093/bioinformatics/btr330

DePristo, M., E. Banks, R. Poplin, K. Garimella, J. Maguire *et al.*, 2011 A framework for variation discovery and genotyping using next-generation DNA sequencing data. Nat. Genet. 43: 491–498. https://doi.org/10.1038/ng.806

Domyan, E., Z. Kronenberg, C. Infante, A. Vickrey, S. Stringham *et al.*, 2016 Molecular shifts in limb identity underlie development of feathered feet in two domestic avian species. eLife 5: e12115. https://doi.org/10.7554/eLife.12115

Drygin, D., A. Siddiqui-Jain, S. O'Brien, M. Schwaebe, A. Lin *et al.*, 2009 Anticancer activity of CX-3543: a direct inhibitor of rRNA biogenesis. Cancer Res. 69: 7653–7661. https://doi.org/10.1158/0008-5472.CAN-09-1304

Frampton, D., H. Schwenzer, G. Marino, L. Butcher, G. Pollara *et al.*, 2018 Molecular signatures of regression of the canine transmissible venereal tumor. Cancer Cell 33: 620–633.e6. https://doi.org/10.1016/j.ccell.2018.03.003

Fu, J., A. Frazee, L. Collado-Torres, A. Jaffe, and J. Leek, 2018 ballgown: Flexible, isoform-level differential expression analysis. R package version 2.14.1, https://rdrr.io/bioc/ballgown/

Garrison, E., 2012 Vcflib: A C++ library for parsing and manipulation VCF files. https://github.com/vcflib/vcflib

Gibson, D., L. Young, R. Chuang, J. Venter, C. Hutchinson *et al.*, 2009 Enzymatic assembly of DNA molecules up to several hundred kilobases. Nat. Methods 6: 343–345. https://doi.org/10.1038/nmeth.1318

Hamede, R., H. McCallum, and M. Jones, 2013 Biting injuries and transmission of Tasmanian devil facial tumour disease. J. Anim. Ecol. 82: 182–190. https://doi.org/10.1111/j.1365-2656.2012.02025.x

Hamede, R., A. Pearse, K. Swift, L. Barmuta, E. Murchison *et al.*, 2015 Transmissible cancer in Tasmanian devils: localized lineage replacement and host population response. Proc. Biol. Sci. 282: 20151468. https://doi.org/10.1098/rspb.2015.1468

Jessy, T., 2011 Immunity over inability: the spontaneous regression of cancer. J. Nat. Sci. Biol. Med. 2: 43–49. https://doi.org/10.4103/0976-9668.82318

Joshi, N. and J. Fass, 2011 Sickle: a sliding-window, adaptive, quality-based trimming tool for FastQ files.

Kim, D., B. Langmead, and S. Salzberg, 2015 HISAT: a fast spliced aligner with low memory requirements. Nat. Methods 12: 357–360. https://doi.org/10.1038/nmeth.3317

Kosack, L., B. Wingelhofer, A. Popa, A. Orlova, B. Agerer *et al.*, 2019 The ERBB-STAT3 axis drives Tasmanian devil facial tumor disease. Cancer Cell 35: 125–139.e9. https://doi.org/10.1016/j.ccell.2018.11.018

Leaché, A., B. Banbury, J. Felsenstein, A. De Oca, and A. Stamatakis, 2015 Short tree, long tree, right tree, wrong tree: new acquisition bias corrections for inferring SNP phylogenies. Syst. Biol. 64: 1032–1047. https://doi.org/10.1093/sysbio/syv053

Li, H., and R. Durbin, 2009 Fast and accurate short read alignment with Burrows-Wheeler Transform. Bioinformatics 25: 1754–1760. https://doi.org/10.1093/bioinformatics/btp324

Lischer, H., and L. Excoffier, 2012 Pgdspider: an automated data conversion tool for connecting population genetics and genomics programs. Bioinformatics 28: 298–299. https://doi.org/10.1093/bioinformatics/btr642

Livak, K., and T. Schmittgen, 2001 Analysis of relative gene expression data using real-time quantitative PCR and the 2(-Delta Delta C(T)) Method. Methods 25: 402–408. https://doi.org/10.1006/meth.2001.1262

Louro, R., H. Nakaya, A. Paquola, E. Martins, A. da Silva *et al.*, 2004 *RASL11A*, member of a novel small monomeric GTPase gene family, is down-regulated in prostate tumors. Biochem. Biophys. Res. Commun. 316: 618–627. https://doi.org/10.1016/j.bbrc.2004.02.091

Magoč, T., and S. Salzberg, 2011 FLASH: fast length adjustment of short reads to improve genome assemblies. Bioinformatics 27: 2957–2963. https://doi.org/10.1093/bioinformatics/btr507

Margres, M., K. Wray, A. Hassinger, M. Ward, J. McGivern *et al.*, 2017 Quantity, not quality: rapid adaptation in a polygenic trait proceeded exclusively through expression differentiation. Mol. Biol. Evol. 34: 3099–3110. https://doi.org/10.1093/molbev/msx231

Margres, M., M. Ruiz-Aravena, R. Hamede, M. Jones, M. Lawrance *et al.*, 2018 The genomic basis of tumor regression in Tasmanian devils (*Sarchophilus harrisii*). Genome Biol. Evol. 10: 3012–3025.

Margres, M., A. Patton, K. Wray, A. Hassinger, M. Ward *et al.*, 2019 Tipping the scales: the migration-selection balance leans toward selection in snake venoms. Mol. Biol. Evol. 36: 271–282. https://doi.org/10.1093/molbev/msy207

McCallum, H., 2008 Tasmanian devil facial tumour disease: lessons for conservation biology. Trends Ecol. Evol. 23: 631–637. https://doi.org/10.1016/j.tree.2008.07.001

McGivern, J., K. Wray, M. Margres, M. Couch, S. Mackessy *et al.*, 2014 RNA-seq and high-definition mass spectrometry reveal the complex and divergent venoms of two rear-fanged colubrid snakes. BMC Genomics 15: 1061. https://doi.org/10.1186/1471-2164-15-1061

McKenna, A., M. Hanna, E. Banks, A. Sivachenko, K. Cibulskis *et al.*, 2010 The Genome Analysis Toolkit: a MapReduce framework for analyzing next-generation DNA sequencing data. Genome Res. 20: 1297–1303. https://doi.org/10.1101/gr.107524.110

McLaren, W., L. Gil, S. Hunt, H. Riat, G. Ritchie *et al.*, 2016 The ensembl variant effect predictor. Genome Biol. 17: 122. https://doi.org/10.1186/s13059-016-0974-4

Metzger, M., A. Villalba, M. Carballal, D. Iglesias, J. Sherry *et al.*, 2016 Widespread transmission of independent cancer lineages within multiple bivalve species. Nature 534: 705–709. https://doi.org/10.1038/nature18599

Miller, M., W. Pfeiffer, and T. Schwartz, 2010 *Creating the CIPRES Science Gateway for Inference of Large Phylogenetic Trees. In 2010 Gateway Computing Environments Workshop*, pp. 1–8 IEEE, New Jersey.

Missotten, G., D. de Wolff-Rouendaal, and R. de Keizer, 2008 Merkel cell carcinoma of the eyelid. review of the literature and report of patients with Merkel cell carcinoma showing spontaneous regression. Ophthalmology 115: 195–201. https://doi.org/10.1016/j.ophtha.2007.02.024

Mittelman, M., D. Neumann, P. Kanter, and N. Haran-Ghera, 2001 Erythropoietin induces tumor regression and antitumor immune responses in murine myeloma models. Proc. Natl. Acad. Sci. USA 98: 5181–5186. https://doi.org/10.1073/pnas.081275298

Morgan, R., M. Dudley, J. Wunderlich, M. Hughes, J. Yang *et al.*, 2006 Cancer regression in patients after transfer of genetically engineered lymphocytes. Science 314: 126–129. https://doi.org/10.1126/science.1129003

Murchison, E., O. Schulz-Trieglaff, Z. Ning, L. Alexandrov, M. Bauer *et al.*, 2012 Genome sequencing and analysis of the Tasmanian devil and its transmissible cancer. Cell 148: 780–791. https://doi.org/10.1016/j.cell.2011.11.065

Murgia, C., J. Pritchard, S. Kim, A. Fassati, and R. Weiss, 2006 Clonal origin and evolution of a transmissible cancer. Cell 126: 477–487. https://doi.org/10.1016/j.cell.2006.05.051

Papac, R., 1998 Spontaneous regression of cancer: possible mechanisms. In Vivo 12: 571–578.

Pearse, A., and K. Swift, 2006 Allograft theory: transmission of devil facial-tumour disease. Nature 439: 549. https://doi.org/10.1038/439549a

Pertea, M., G. Pertea, C. Antonescu, T. Chang, J. Mendell *et al.*, 2015 StringTie enables improved reconstruction of a transcriptome from RNA-seq reads. Nat. Biotechnol. 33: 290–295. https://doi.org/10.1038/nbt.3122

Pertea, M., D. Kim, G. Perea, J. Leek, and S. Salzberg, 2016 Transcript-level expression analysis of RNA-seq experiments with HISAT, StringTie and Ballgown. Nat. Protoc. 11: 1650–1667. https://doi.org/10.1038/nprot.2016.095

Pistoni, M., A. Verrecchia, M. Doni, E. Guccione, and B. Amati, 2010 Chromatin association and regulation of rDNA transcription by the Ras-family protein RasL11a. EMBO 29: 1215–1224. https://doi.org/10.1038/emboj.2010.16

Pye, R., R. Hamede, H. Siddle, A. Caldwell, G. Knowles *et al.*, 2016a Demonstration of immune responses against devil facial tumour disease in wild Tasmanian devils. Biol. Lett. 12: 20160553. https://doi.org/10.1098/rsbl.2016.0553

Pye, R., D. Pemberton, C. Tovar, J. Tubio, K. Dun *et al.*, 2016b A second transmissible cancer in Tasmanian devils. Proc. Natl. Acad. Sci. USA 113: 374–379. https://doi.org/10.1073/pnas.1519691113

Rambaut, A., 2012 *FigTree v1.4. Molecular Evolution, Phylogenetic, and Epidemiology*, University of Edinburgh, Institute of Evolutionary Biology, Edinburgh, UK.

Roche, B., B. Arcangioli, and R. Martienssen, 2017 New roles for Dicer in the nucleolus and its relevance to cancer. Cell Cycle 16: 1643–1653. https://doi.org/10.1080/15384101.2017.1361568

Sanchez-Vega, F., M. Mina, J. Armenia, W. Chatila, A. Luna *et al.*, 2018 Oncogenic signaling pathways in the cancer genome atlas. Cell 173: 321–337.e10. https://doi.org/10.1016/j.cell.2018.03.035

Sengupta, N., T. MacFie, T. MacDonald, D. Pennington, and A. Silver, 2010 Cancer immunoediting and "spontaneous" tumor regression. Pathol. Res. Pract. 206: 1–8. https://doi.org/10.1016/j.prp.2009.10.001

Sharma, P., S. Hu-Lieskovan, J. Wargo, and A. Ribas, 2017 Primary, adaptive, and acquired resistance to cancer immunotherapy. Cell 168: 707–723. https://doi.org/10.1016/j.cell.2017.01.017

Stamatakis, A., 2014 RAxML version 8: a tool for phylogenetic analysis and post-analysis of large phylogenies. Bioinformatics 30: 1312–1313. https://doi.org/10.1093/bioinformatics/btu033

Stammnitz, M., T. Coorens, K. Gori, D. Hayes, B. Fu *et al.*, 2018 The origins and vulnerabilities of two transmissible cancers in Tasmanian Devils. Cancer Cell 33: 607–619.e15. https://doi.org/10.1016/j.ccell.2018.03.013

Stelzer, G., R. Rosen, I. Plaschkes, S. Zimmerman, M. Twik *et al.*, 2016 The GeneCards suite: from gene data mining to disease genome sequence analyses. *Curr. Protoc Bioinformatics* 54. https://doi.org/10.1002/cpbi.5

Storfer, A., P. Hohenlohe, M. Margres, H. McCallum, A. Patton *et al.*, 2018 The devil is in the details: genomics of transmissible cancers in tasmanian devils. PLoS Pathog. 14: e1007098. https://doi.org/10.1371/journal.ppat.1007098

Sukumaran, J., and M. Holder, 2010 Dendropy: a python library for phylogenetic computing. Bioinformatics 26: 1569–1571. https://doi.org/10.1093/bioinformatics/btq228

Swofford, D. L., 1998 *Phylogenetic Analysis Using Parsimony* (PAUP*), version 4.0*, Sinauer Associates, Sunderland, MA.

Vogelstein, B., N. Papadopoulos, V. Velculescu, S. Zhou, L. Diaz, Jr. *et al.*, 2013 Cancer genome landscapes. Science 339: 1546–1558. https://doi.org/10.1126/science.1235122

Wangsa, D., R. Braun, C. Stuelten, M. Brown, K. Bauer *et al.*, 2019 Induced chromosomal aneuploidy results in global and consistent deregulation of the transcriptome of cancer cells. Neoplasia 21: 721–729. https://doi.org/10.1016/j.neo.2019.04.009

Way, G., F. Sanchez-Vega, K. La, J. Armenia, W. Chatila *et al.*, 2018 Machine learning detects pan-cancer ras pathway activation in the cancer genome atlas. Cell Rep. 23: 172–180.e3. https://doi.org/10.1016/j.celrep.2018.03.046

Weber, M., J. Davies, D. Wittig, E. Oakeley, M. Haase *et al.*, 2005 Chromosome-wide and promoter-specific analyses identify sites of differential DNA methylation in normal and transformed human cells. Nat. Genet. 37: 853–862. https://doi.org/10.1038/ng1598

Wright, B., C. Willet, R. Hamede, M. Jones, K. Belov *et al.*, 2017 Variants in the host genome may inhibit tumour growth in devil facial tumours: evidence from genome-wide association. *Sci. Rep.* 7: 423. https://doi.org/10.1038/s41598-017-00439-7

Communicating editor: S. Sharan